Control of Loudspeakers Using Disturbance-Observer-Type Velocity Estimation

Yaoyu Li, *Member, IEEE,* and George T.-C. Chiu, *Member, IEEE*

***Abstract*—In this paper, a new approach to obtain sensorless velocity feedback for loudspeakers is developed. The back electromotive force (back-EMF) of the moving coil is estimated by using a disturbance-observer-type estimator based on the coil current measurement. The cone velocity of a loudspeaker can be obtained based on its proportionality to the back-EMF. Instead of relying on the coupled mechanical dynamics as reported in previous work, the proposed velocity estimation is based on the precise knowledge of electrical impedance, which makes it more robust to changes in acoustic loading. The proposed approach enables the development of a robust velocity controller for a subwoofer without an expensive velocity measuring device. Experimental results demonstrated that closed-loop velocity control using the proposed scheme of velocity estimation achieved a performance comparable to that obtained by using measured velocity feedback. The proposed approach can be easily adapted to other moving-coil-type linear actuators.**

***Index Terms*—Disturbance observer, loudspeaker, sensorless control, velocity estimation.**

I. Introduction

In ACOUSTIC control applications such as active noise control and audio systems, the loudspeaker is the most commonly used actuator. In most analysis for acoustic control systems, the actuation is usually assumed to be a constant volume velocity source and the actual actuator dynamics are often neglected. A constant volume velocity source should generate a constant diaphragm velocity for constant input within the desirable operating frequency range. This implies that a desirable velocity frequency response for an ideal acoustical actuator should exhibit a bandpass behavior where the passband is the desired operating frequency range, and the magnitude and phase of the frequency response should be constant within the passband. A well-designed loudspeaker behaves like a bandpass filter. However, its velocity frequency response usually contains frequency-dependent magnitude and phase (see Fig. 1). It is well known that the passband frequency range as well as the frequency-dependent magnitude and phase of the loudspeaker velocity frequency response are the results of the interaction between loudspeaker dynamics and its environment.

The major mechanical parts for a typical moving-coil loudspeaker are diaphragm and suspension. The diaphragm is considered to be a moving mass, while the suspension along with its acoustic load, e.g., its enclosure, provides the compliance for the actuator [1]. At low frequencies, the diaphragm oscillates like a piston and displaces a volume of air that is proportional to the displacement of the diaphragm. This mode of operation is sometimes referred to as the piston mode of the loudspeaker. As the frequency of excitation increases, the diaphragm does not respond as a rigid piston but as a flexible structure where higher order modes start to affect the diaphragm response. In the piston mode, the loudspeaker can be modeled as a mass-spring-damper system. The electromagnetic force generated by driving current through the motor coil of the speaker is the force acting on the mass.

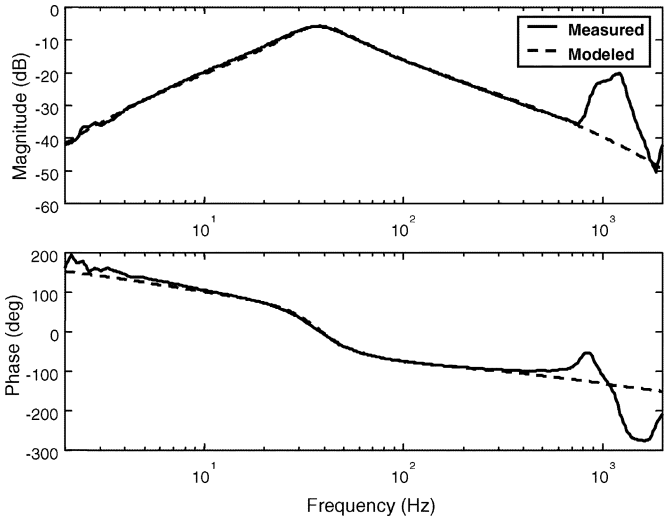

Fig. 1. Velocity frequency response of a subwoofer loudspeaker.

Fig. 2(a) shows the functional block diagram of a moving-coil loudspeaker operating in the piston mode. $U(s)$, $E_b(s)$, and $I(s)$ are the applied voltage, the back electromotive force (back-EMF), and the motor coil current, respectively. $F(s)$ and $v(s)$ are the electromagnetic force applied to the diaphragm piston and the resulting piston (diaphragm) velocity, respectively. The parameters L and R denote the inductance and resistance of the motor coil, respectively. The parameter Bl represents the force/back-EMF constant of the moving-coil motor. The mechanical impedance of the diaphragm can be expressed as $s/(ms^2+bs+k)$, where the parameters m, b, and k are the effective mass, damping coefficient, and stiffness of the combined mechanical system of the speaker and the surrounding environment, respectively.

Manuscript received August 7, 2003; revised April 23, 2004.

Y. Li is with the Ray W. Herrick Laboratories, School of Mechanical Engineering, Purdue University, West Lafayette, IN 47907-2031 USA (e-mail: liyaoyu@ecn.purdue.edu).

G. T.-C. Chiu is with the School of Mechanical Engineering, Purdue University, West Lafayette, IN 47907-1288 USA (e-mail: gchiu@ecn.purdue.edu).

Digital Object Identifier 10.1109/TMECH.2004.842215

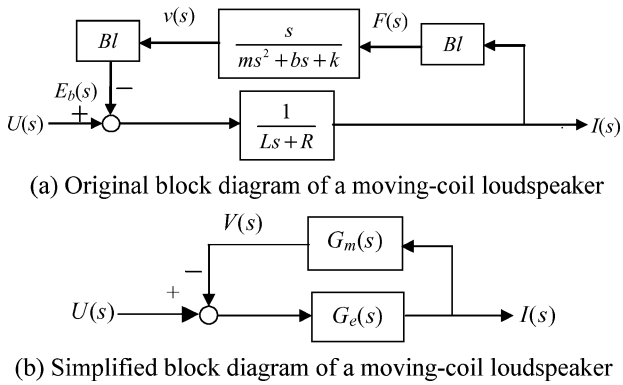

(a) Original block diagram of a moving-coil loudspeaker

(b) Simplified block diagram of a moving-coil loudspeaker

Fig. 2. Block diagrams of the piston-mode operation of a moving-coil loudspeaker.

A significant amount of work has been done to improve the performance and to minimize the distortion of loudspeakers [2]–[5]. Most of these works revolve around the design of the loudspeaker, the design of the speaker enclosure, and some form of motional feedback that requires additional sensors. To improve loudspeaker response for acoustic control applications, the velocity frequency response of the loudspeaker with respect to the input voltage of the audio amplifier (see Fig. 1) should look like that of a bandpass filter with flat (constant magnitude) passband response. Motional feedback control techniques can be used to achieve the desirable response. To implement motional control, information regarding the motion of the diaphragm, e.g., acceleration, velocity, or displacement, is required as the feedback signal. To improve loudspeaker velocity response, the speaker diaphragm velocity is an obvious choice for feedback. There are two approaches to obtaining loudspeaker diaphragm velocity. One is to attach velocity transducers to the speaker [3], [6]–[8], and the other is to estimate diaphragm velocity [9]–[11]. Physically attaching transducers such as accelerometers, microphones, or laser vibrometers requires additional hardware, which tends to increase the speaker mass as well as the cost of the overall system. The additional sensor may also be intrusive to the overall acoustic system. Two methods of estimating diaphragm velocity have been proposed. One approach is to exploit the proportionality between the back-EMF signal $E_b(s)$ and the diaphragm velocity [9], [11]. The other is to construct a velocity observer by measuring the coil current $I(s)$ [10]. The coil current can be more cost-effectively obtained than the back-EMF signal in an actively driven coil.

Lane and Clark [10] presented a simple but effective approach to estimate loudspeaker diaphragm velocity from the coil current measurement. Their approach is similar to building an open-loop reduced order observer, in which an accurate model of the mechanical dynamics of the loudspeaker is required to obtain the desired velocity estimation. In this paper, we will present an approach that uses the disturbance-observer concept in estimating the diaphragm velocity for feedback control [12]. The proposed approach is similar to the method described in [10] in that both methods use the coil current to estimate the diaphragm velocity. However, unlike the method described in [10], the proposed estimation approach is based on the precise knowledge of electrical impedance of the actuator instead of the coupled mechanical dynamics of the loudspeaker and its environment. This feature also distinguishes the proposed method from that of using a closed-loop observer to recover the velocity information from coil current measurement. A controller can be designed for a specific speaker without precise knowledge of the external loading condition and still maintain a constant volume velocity response in a prescribed frequency range. Experimental results using the proposed approach show a closed-loop performance comparable to the closed-loop control using actual measured velocity feedback.

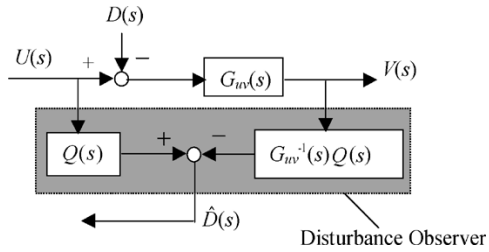

Fig. 3. Disturbance-observer structure.

The remainder of the paper is organized as follows. The structure and design of disturbance-observer-based velocity estimation is discussed in Section II. The sensitivity analysis on both the proposed approach and the method from [10] are then given along with simulation results, followed by the stability analysis using the proposed velocity estimation in closed-loop control. Experimental results are presented in Section III. Conclusions and future work will be discussed in Section IV.

II. Disturbance-Observer-Type Velocity Estimation

In this section, the design and analysis of disturbance-observer-based velocity estimation will be discussed. We will first review the disturbance-observer concept and then extend it to the estimation of loudspeaker diaphragm velocity. The design of the proposed velocity estimation approach will then be presented. For both the proposed approach and the approach in [10], the sensitivity of the velocity estimation with respect to the mechanical impedance will be examined, and a simulation study will be conducted for nominal and perturbed mechanical impedance.

A. Velocity Estimator Structure

The concept of a disturbance observer was originally proposed to compensate for external disturbance [13]–[15], e.g., friction and torque ripple, in electromechanical motion control applications. The basic structure of a disturbance observer is illustrated in Fig. 3. The only design parameter in the disturbance observer is the filter $Q(s)$, which must have a relative degree such that $G_{uv}^{-1}(s)Q(s)$ is proper. From Fig. 3, we see that the relative estimation error between the actual disturbance $D(s)$ and the estimated disturbance $\hat{D}(s)$ is

$$\frac{D(s)-\hat{D}(s)}{D(s)} = 1 - Q(s). \tag{1}$$

Therefore, the filter $Q(s)$ is often selected to be a low-pass filter with gain close to 1 in the frequency range where precise estimation is desired.

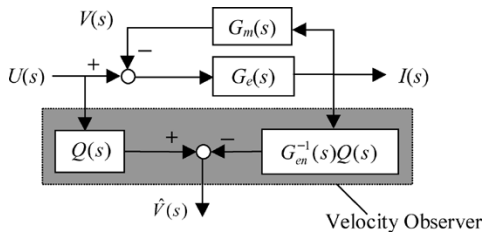

Fig. 4. Disturbance-observer-type velocity estimator.

Without loss of generality, the block diagram for the loudspeaker shown in Fig. 2(a) can be simplified into the diagram in Fig. 2(b), where $G_e(s) = 1/(Ls + R)$ represents the electrical impedance and $G_m(s) = (Bl)^2 s/(ms^2 + bs + k)$ represents the mechanical impedance, respectively. Here $V(s)$ denotes a scaled velocity signal, i.e., the back-EMF $E_b(s)$. When comparing Fig. 3 with Fig. 2(b), the signal $V(s)$ can be treated as a "disturbance" input to the electrical part of the system, and then the concept of disturbance observer can be used to estimate $V(s)$.

Fig. 4 shows the structure of the proposed velocity estimator (observer), where the nominal electrical impedance of the loudspeaker is denoted by $G_{en}(s)$ and the actual electrical impedance is denoted by $G_e(s)$. Note that the filter $Q(s)$ plays a similar role as the Q-filter in the disturbance observer. Note also that the proposed velocity estimator does not depend on the mechanical impedance $G_m(s)$. The structure of the velocity estimator has the advantage that it does not require additional sensor on the load (mechanical) side of the loudspeaker. Since only the applied voltage $U(s)$ and the coil current $I(s)$ is needed, this estimator is ideal for modular design, where the controller is embedded with the speaker and tuned before it is integrated into the acoustic control system.

B. Sensitivity Analysis of Closed-Loop Control Using Velocity Estimation

The sensitivity function of velocity estimation $\hat{V}(s)$ with respect to the perturbation in $G_m(s)$ indicates the change of the estimation with the variation of the mechanical impedance. From Fig. 4, in the case of disturbance-observer-type velocity observer, the velocity estimation is

$$\hat{V}(s) = U(s)Q(s) - \frac{G_e(s)G_{en}^{-1}(s)Q(s)U(s)}{1 + G_e(s)G_m(s)} \tag{2}$$

and the sensitivity function is

$$S_{G_m}^{\hat{V},d}(s) = \frac{\partial \hat{V}(s)}{\partial G_m(s)} \frac{G_m(s)}{\hat{V}(s)}. \tag{3}$$

The superscript d denotes that it is the sensitivity function for the *disturbance-observer-type estimation*. Substituting (2) into (3), and after some derivation, it becomes

$$S_{G_m}^{\hat{V},d}(s) = \frac{G_{en}^{-1}(s)G_e^2(s)G_m(s)}{[1 + G_e(s)G_m(s)]\,[1 + G_e(s)G_m(s) - G_{en}^{-1}(s)G_e(s)]}. \tag{4}$$

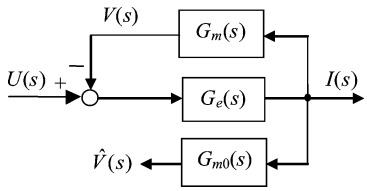

Fig. 5. Velocity estimation scheme proposed by Lane and Clark [10].

Assuming a good estimation of the electrical impedance, i.e., $G_{en}(s) \cong G_e(s)$, the above equation can be simplified to

$$S_{G_m}^{\hat{V},d}(s) = \frac{1}{1 + G_e(s)G_m(s)}. \tag{5}$$

To show the robustness of the above velocity estimation to the variation of mechanical impedance, we consider the sensitivity function of the velocity estimation with respect to the mechanical impedance for the method developed in [10]. Fig. 5 shows their estimation scheme. The basic idea is to filter the current output with the mechanical impedance model of the loudspeaker. The velocity estimation in [10] is

$$\hat{V}(s) = \frac{G_e(s)G_{m0}(s)}{1 + G_e(s)G_m(s)} U(s) \tag{6}$$

where the nominal mechanical impedance

$$G_{m0}(s) = \frac{(Bl)^2 s}{m_0 s^2 + b_0 s + k_0} \tag{7}$$

is used to filter the current output. The nominal mechanical mass, damping, and stiffness are denoted by m_0, b_0, and k_0, respectively, which are constant regardless of the variation of mechanical impedance. The sensitivity of this velocity estimation with respect to $G_m(s)$ is given by

$$S_{G_m}^{\hat{V},i}(s) = \frac{\partial \hat{V}(s)}{\partial G_m(s)} \frac{G_m(s)}{\hat{V}(s)} \tag{8}$$

where superscript i is used to differentiate this method from the disturbance observer approach. Substituting (6) into (8), we obtain

$$S_{G_m}^{\hat{V},i}(s) = -\frac{G_e(s)G_m(s)}{1 + G_e(s)G_m(s)}. \tag{9}$$

If the proposed disturbance-observer-type velocity estimator is more robust than the scheme in [10] with respect to the change of mechanical impedance, we have $\|S_{G_m}^{\hat{V},i}(s)\|_\infty > \|S_{G_m}^{\hat{V},d}(s)\|_\infty$. If (5) is compared with (9), it is equivalent to considering whether or not the following is valid:

$$\|G_e(s)G_m(s)\|_\infty > 1. \tag{10}$$

Since

$$\|G_e(s)G_m(s)\|_\infty \geq \left| \frac{1}{(Ls + R)} \frac{(Bl)^2 s}{(ms^2 + bs + k)} \right|_{s = j\omega_n} \tag{11}$$

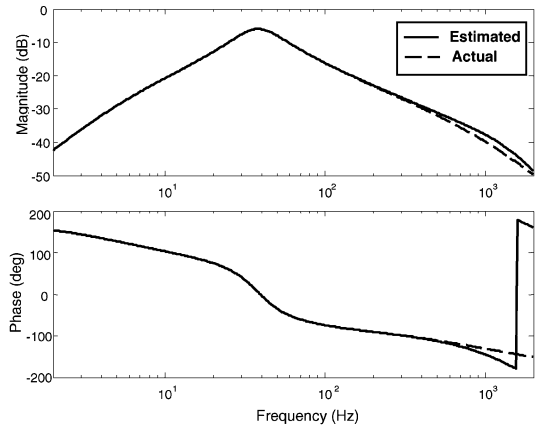

(a) Disturbance observer scheme of velocity estimation for nominal mechanical impedance

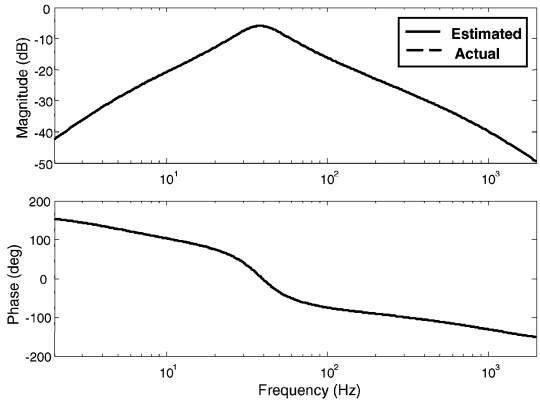

(b) Velocity estimation scheme in [10] for nominal mechanical impedance

Fig. 6. Comparison of velocity estimation for nominal mechanical impedance.

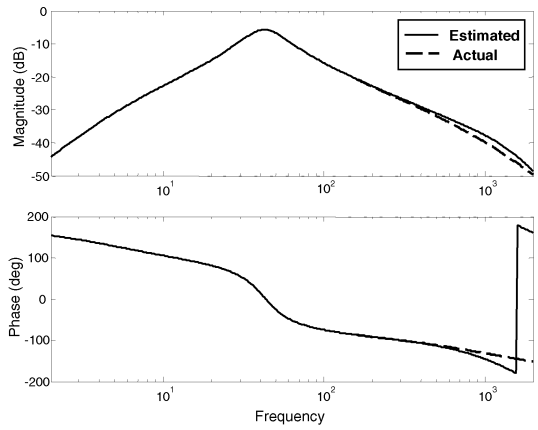

(a) Disturbance observer scheme of velocity estimation for perturbed mechanical impedance

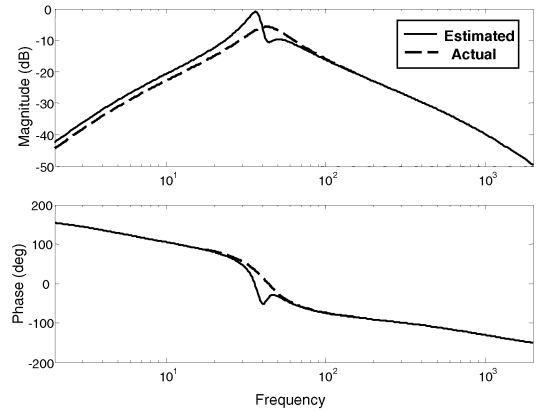

(b) Velocity estimation scheme in [10] for perturbed mechanical impedance

Fig. 7. Comparison of velocity estimation for perturbed mechanical impedance.

where $\omega_n = \sqrt{k/m}$ is the natural frequency for the mechanical impedance, a simplified treatment is to verify if the right-hand side of inequality (11) is greater than 1. Since

$$\left|\frac{1}{(Ls+R)}\frac{(Bl)^2 s}{(ms^2+bs+k)}\right|_{s=j\omega_n} = \frac{(Bl)^2}{b}\frac{1}{\left|jL\sqrt{\frac{k}{m}}+R\right|} = \frac{(Bl)^2}{bR}\frac{1}{\sqrt{1+\frac{k}{m}\frac{L}{R}}} \tag{12}$$

where the electrical time constant L/R, the mechanical resistance coefficient b and coil resistance R are small for most loudspeakers, $\|G_e(s)G_m(s)\|_\infty > 1$ is possible. For instance, for a typical subwoofer similar to the one used in this research, $Bl =$ 6 N/A, $R = 4\ \Omega$, $b = 1.5$ N $\cdot$ s/m, $L = 1$ mH, $\omega_n = 80\pi$ rad/s, we have

$$\frac{(Bl)^2}{bR}\frac{1}{\sqrt{1+\frac{k}{m}\frac{L}{R}}} = 1.46 > 1.$$

The two velocity estimation schemes are also compared via simulation study. For the estimated plant model used later in Section III, the simulated frequency responses of velocity estimation using the disturbance-observer scheme and the framework in [10] are shown in Fig. 6, respectively, assuming that the mechanical impedance is known. For the scheme in [10], since the current output is filtered by the exact mechanical impedance, perfect estimation is obtained for all frequencies. While the disturbance-observer scheme cannot provide good estimation above 400 Hz because of the limited bandwidth of $Q(s)$, the performance for low- to mid-frequency range is acceptable.

Simulation is repeated for the case where the stiffness of the mechanical impedance is increased by 25% intentionally, as shown in Fig. 7. Either using an enclosure smaller than the nominal or some increase in diaphragm stiffness can result in such a change. The simulation results show that the estimation performance of the disturbance-observer method was barely affected, while the estimation using the method in [10] became quite distorted in the passband, especially around the mechanical resonance.

In summary, the sensitivity analysis and simulation results have shown that the proposed disturbance observer scheme of velocity estimation is more robust to the change of mechanical impedance.

C. Stability Analysis on a Closed-Loop System

Velocity feedback is used to achieve closed-loop control. If velocity measurement is available, a stabilizing controller $C(s)$

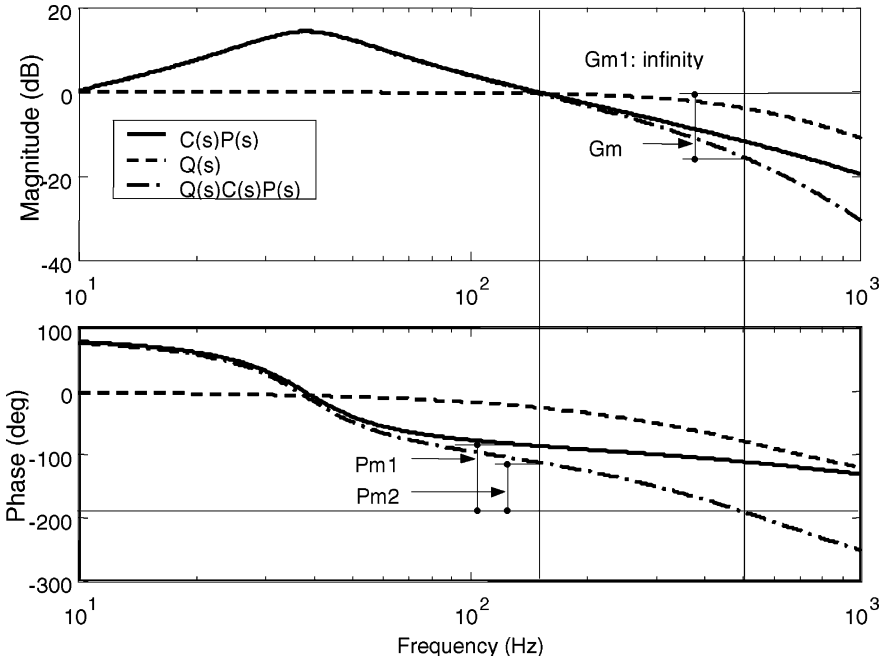

Fig. 8. Stability margins of closed-loop systems with measured and estimated velocity feedback.

can be designed. However, closed-loop stability needs to be studied when the same controller is applied to the system with the proposed velocity estimation as feedback.

Assume $C(s)$, $G_e(s)$, and $G_m(s)$ are proper and stable transfer functions. If the actual velocity measurement is available, the closed-loop transfer function from $U(s)$ to $V(s)$ is

$$G_{CL1}(s) = \frac{C(s)G_e(s)G_m(s)}{1 + G_e(s)G_m(s) + C(s)G_e(s)G_m(s)}. \quad (13)$$

For the case of the proposed velocity estimator, the transfer function from $U(s)$ to $V(s)$ is

$$G_{CL2}(s) = \frac{C(s)G_e(s)G_m(s)}{1 + G_e(s)G_m(s) + C(s)Q(s)G_e(s)G_m(s)} \quad (14)$$

with $G_{en}(s) \cong G_e(s)$. Based on this, divide both the numerator and the denominator for the right-hand side of (14) by $[1 + G_e(s)G_m(s)]$ as follows:

$$G_{CL2}(s) = \frac{C(s)\frac{G_e(s)G_m(s)}{1+G_e(s)G_m(s)}}{1 + Q(s)C(s)\frac{G_e(s)G_m(s)}{1+G_e(s)G_m(s)}}. \quad (15)$$

Let $P(s) = G_e(s)G_m(s)/(1 + G_e(s)G_m(s))$, and then (14) can be simplified to

$$G_{CL2}(s) = \frac{C(s)P(s)}{1 + Q(s)C(s)P(s)}. \quad (16)$$

In (16), $Q(s)$ can be considered as the sensor dynamics for the equivalent plant $P(s)$. The effect of $Q(s)$ on stability margins is illustrated in Fig. 8. The Bode plots of $C(s)P(s)$ and $Q(s)$ are plotted, respectively. The Bode plot of the new loop transfer function $C(s)P(s)Q(s)$ can be obtained by simple superposition of the corresponding magnitude and phase responses. As mentioned in the previous section, the filter $Q(s)$ is often selected to be a low-pass filter with gain close to 1 in the frequency range where precise estimation is desired. Low-pass filters will introduce phase lag that is small for low frequencies but increases for high frequencies. Due to the addition of $Q(s)$, the phase margin and gain margin of the closed-loop system will be reduced. A good choice of $Q(s)$ should introduce little phase lag within the performance region. This requires the bandwidth of $Q(s)$ to be large, which has to be traded off with adequate noise suppression and computation resource.

III. Experimental Results

To verify the proposed velocity estimation feedback, experiments were conducted using a Radio Shack 20-cm-diameter 50-W subwoofer as specified in [11] and [12]. The QSC-1100 audio amplifier is used to provide needed power to the voice coil. The subwoofer is installed in the aperture centered on a 1.8 m×1.8 m plywood board. The board is erected in an anechoic chamber. The input signals were generated by an HP35670 Dynamic Signal Analyzer. The cone velocity was measured with a laser vibrometer. The voltage signal of the vibrometer that is proportional to the diaphragm velocity was sent back to the analyzer to obtain the open-loop velocity response.

The measured open-loop velocity response is shown in Fig. 1. Nominally, the velocity response is supposed to be a third-order system (see Fig. 2) with the following transfer function:

$$G_{wv}(s) = \frac{k_a Bl\, s}{Lms^3 + (Rm + bL)s^2 + \left[Rb + kL + (Bl)^2\right] s + Rk}. \quad (17)$$

The third-order model fits well in the mid-frequency range, but is not as accurate for a lower frequency range due to the additional dynamics of the audio amplifier. The audio amplifier was

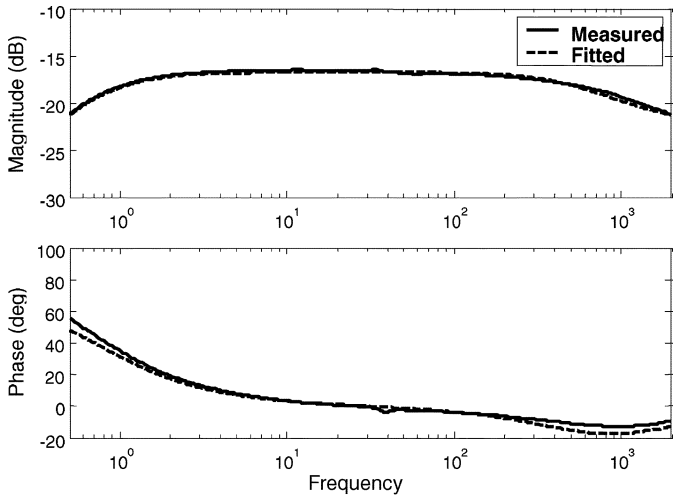

Fig. 9. Measured frequency response of $G_e(s)$ and its fitting.

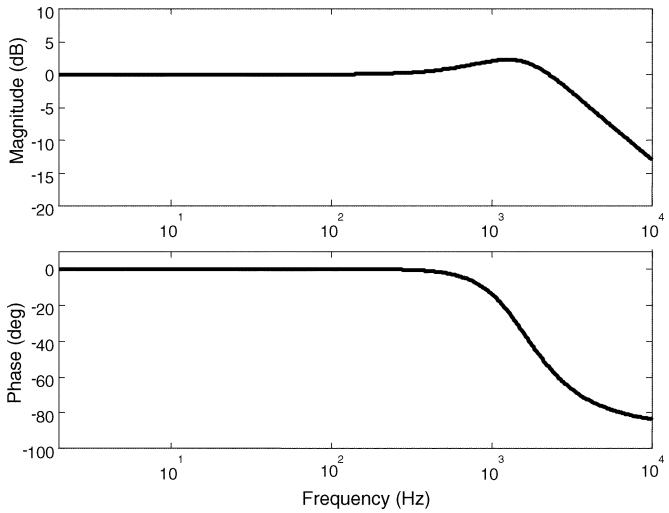

Fig. 10. Frequency response of the low-pass filter $Q(s)$.

found to have the dynamics $K(s) = (3.622\ s + 0.6492)/(s + 29.49)$. By incorporating the amplifier dynamics, a fourth-order model was obtained as follows:

$$\hat{G}_{uv}(s) = \frac{611\,678\ s\,(s+0.1792)}{(s^2+173.1s+5.725\times 10^4)(s+6775)(s+29.49)}. \tag{18}$$

Since a precise model of $G_e(s)$ is important for good estimation, the frequency response of electrical impedance $G_e(s)$ was measured using the following approach. To measure the electrical impedance $G_e(s)$, we need to obtain the corresponding input and output signals. The output signal is the current of the voice coil, and the input is the difference between $U(s)$ and the back-EMF $E_b(s)$. The input voltage $U(s)$ and the velocity signal from the vibrometer are sent to the two A/D ports of a DSP system and the subtraction was done in real time. The subtraction result $U(s) - BlV(s)$ and the current signal $I(s)$ are then compared in the spectrum analyzer to obtain the frequency response of $G_e(s)$. The measurement results and its fitted response are shown in Fig. 9. The fitted model for $G_e(s)$ is

$$\hat{G}_e(s) = \frac{0.078\,23(s+7414)(s+0.3142)}{(s+3990)(s+4.273)}. \tag{19}$$

Note that the nominal electrical impedance of the voice coil is $1/(Ls + R)$, i.e., a first-order low-pass model. The actual response is similar to the nominal model for mid-frequency range but is augmented by the audio amplifier at low frequencies. Since the inductance L decreases at high frequencies, this accounts for the high-frequency zero.

The mechanical part of the system (velocity response) is used in identifying the electrical impedance $G_e(s)$. In actual implementation, the mechanical characteristics of the system are highly coupled to the operating environment, while $G_e(s)$ is much less dependent on the operating environment. With this approach, the estimated velocity will be less likely affected by different operating environment, and the estimator will not need to be recalibrated if the operating environment changes.

The fitted model of $\hat{G}_e(s)$ was used as the nominal model $G_{en}(s)$. The method described in Fig. 4 was then applied to estimate the velocity. A modified second-order Butterworth filter was used as the Q filter as follows:

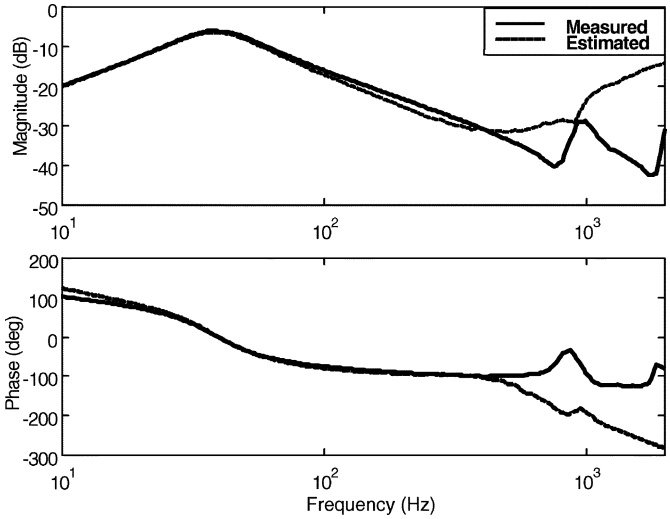

Fig. 11. Disturbance-observer-type velocity estimation for an open-air subwoofer.

$$Q(s) = \frac{13\,988(s+6974.3)}{s^2+1.403\times 10^4 s+9.756\times 10^7}. \tag{20}$$

A zero at about 1.1 kHz is added to improve phase response for the frequencies up to 400 Hz. Fig. 10 shows the frequency response of the designed Q-filter. The actual frequency response from the input voltage $U(s)$ to the estimation $\hat{V}(s)$ is shown in Fig. 11. Velocity estimation was good from 10 to approximately 400 Hz. As a constant velocity source is often preferred in acoustics applications, a fourth-order robust controller was designed via a loop-shaping method [16] to achieve a relatively flat velocity response for the subwoofer.

Fig. 12 shows the closed-loop responses as compared with the open-loop response. The closed-loop velocity responses were obtained using the same controller with the actual velocity measurement of a laser vibrometer and with the proposed velocity estimation, respectively. The closed-loop velocity responses were very close for 2–200 Hz between using direct

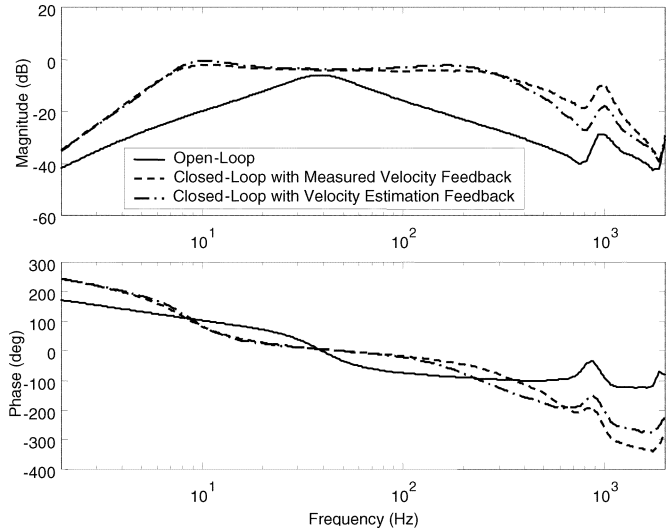

Fig. 12. Comparison of open-loop and closed-loop velocity responses.

velocity feedback and disturbance-observer-type velocity estimation. Within ±3-dB magnitude fluctuation, the closed-loop system using disturbance-observer-type velocity estimation achieved a passband approximately from 7 to about 300 Hz. The discrepancy increases as the frequency approaches to the limitation of the velocity estimation, i.e., around 400 Hz.

IV. Conclusion and Discussion

A disturbance-observer-type velocity estimator was developed for moving-coil type linear actuators based on the precise knowledge of the electrical impedance of the actuator. Without relying on the precise knowledge of the dynamics of the mechanical impedance, the proposed approach is more applicable to a varying environment. Back-EMF of the linear actuator is treated as an external disturbance that is applied to the input end of the electrical impedance of the linear actuator. The proposed approach was shown to be more robust to the variation of mechanical impedance than the velocity estimation scheme in [10] via the sensitivity analysis and simulation study. The stability of the closed-loop system using the proposed estimation scheme revealed the important role of the Q-filter. Experiments were done for an open-air subwoofer, and good velocity estimation was obtained for 10–400 Hz. Closed-loop control using the estimated velocity feedback demonstrated similar performance with measured velocity feedback. The proposed velocity estimation approach can be extended to other moving-coil-type actuators.

References

[1] M. Colloms, *High Performance Loudspeakers*. London, U.K.: Wiley, 1997.
[2] R. L. Tanner, "Improving loudspeaker response with motional feedback," *Electron.*, vol. 142, pp. 228–240, 1951.
[3] R. A. Greiner and T. M. Sims Jr., "Loudspeaker distortion reduction," *J. Audio Eng. Soc.*, vol. 32, pp. 956–963, 1984.
[4] P. G. L. Mills and M. O. J. Hawksford, "Distortion reduction in moving-coil loudspeaker systems using current-drive technology," *J. Audio Eng. Soc.*, vol. 37, pp. 129–148, 1989.
[5] J. Suykens, J. Vandewalle, and J. Van Ginderdeuren, "Feedback linearization of nonlinear distortion in electrodynamics loudspeaker," *J. Audio Eng. Soc.*, vol. 43, pp. 690–694, 1995.
[6] D. De Greef and J. Vandewege, "Acceleration feedback loudspeaker," *Wireless World*, pp. 32–36, 1981.
[7] M. A. Khalid and A. Packard, "Control of closed-box loudspeaker systems," in *Proc. IFAC 13th Triennial World Congress*, 1996, pp. 481–486.
[8] D. Hall, "Loudspeaker with Motional Feedback," U.S. Patent 4 727 584, 1988.
[9] C. J. Radcliffe, S. D. Gogate, and G. Hall, "Development of an active acoustic sink for noise control applications," in *Proc. 1994 ASME Winter Annu. Meetings—Active Contr. Vibration Noise*, vol. 75, 1994, pp. 43–50.
[10] S. A. Lane and R. L. Clark, "Improving loudspeaker performance for active noise control applications," *J. Audio Eng. Soc.*, vol. 46, pp. 508–519, 1998.
[11] C. Y. Chen, C. C. Cheng, G. T.-C. Chiu, and H. Peng, "Passive voice-coil feedback control of closed-box subwoofer systems," *J. Mech. Eng. Sci. C*, vol. 214, pp. 995–1005, 2000.
[12] Y. Li and G. T.-C. Chiu, "Control of loudspeakers using disturbance-observer type velocity estimation for noise and vibration control," in *Proc. 2000 Japan-USA Symp. Flexible Automat.*, vol. 2, 2000, pp. 913–919.
[13] K. Ohnishi, "A new servo method in mechatronics," *Trans. Jpn. Soc. Elect. Eng.*, vol. 107-D, pp. 83–86, 1987.
[14] T. Umeno and Y. Hori, "Robust speed control of DC servomotors using modern two degrees-of-freedom controller design," *IEEE Trans. Ind. Electron.*, vol. 38, no. 5, pp. 363–368, Oct. 1991.
[15] E. Schrijver and J. van Dijk, "Disturbance observers for rigid mechanical systems: Equivalence, stability, and design," *ASME J. Dynam. Syst., Meas. Contr.*, vol. 124, no. 4, pp. 539–548, 2002.
[16] J. C. Doyle, B. A. Francis, and A. Tannenbaum, *Feedback Control Theory*. New York: Macmillan, 1990.

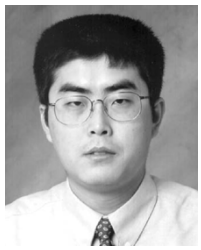

Yaoyu Li (M'04) received the B.Sc. degree in mechatronics from Tsinghua University, Beijing, China, in 1992, the M.Sc. degree in engineering from the University of Saskatchewan, Saskatoon, SK, Canada, in 1997, and the Ph.D. degree in mechanical engineering from Purdue University, West Lafayette, IN, in 2004.

He is now an Assistant Professor with the Department of Mechanical Engineering, University of Wisconsin, Milwaukee. From 1992 to 1994, he was an Assistant Research Engineer with the Inner Mongolia Institute of Microcomputer Technology, Hohhot, Inner Mongolia, China. He joined the University of Wisconsin at Milwaukee, in July 2004. His recent research interests include robust and adaptive control in acoustics and vibration and extremum seeking control with application to tunable thermoacoustic coolers.

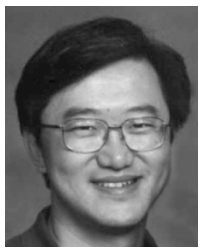

George T.-C. Chiu (M'02) received the B.S. degree from National Taiwan University, Taipei, Taiwan, in 1985 and the M.S. and Ph.D. degrees from the University of California, Berkeley, in 1990 and 1994, respectively, all in mechanical engineering.

He is an Associate Professor with the School of Mechanical Engineering, Purdue University, West Lafayette, IN. From 1994 to 1996, he was a Research and Development Engineer with Hewlett-Packard, developing high-performance color inkjet printers and multifunction machines. He joined Purdue University in 1996. His current research interests are modeling and control of digital imaging and printing systems, motion and vibration control, mechatronics, and adaptive and optimal control.

Prof. Chiu is a member of the American Society of Mechanical Engineers (ASME) and the Society of Imaging Science and Technology (IS&T). He is currently the chair of the Adaptive and Optimal Control Panel of the ASME Dynamic Systems and Control Division.